CONTRAST MEDIA & MOLECULAR IMAGING

Received: 2 May 2012, Revised: 2 July 2012, Accepted: 27 July 2012, Published online in Wiley Online Library: 2012

(wileyonlinelibrary.com) DOI: 10.1002/cmmi.1494

Field dependence of T_1 for hyperpolarized [1-^{13}C]pyruvate

N. Chattergoon[a], F. Martínez-Santiesteban[a,b], W. B. Handler[c], J. H. Ardenkjær-Larsen[d,e] and T. J. Scholl[a,b]*

In vivo **metabolism of hyperpolarized pyruvate has been demonstrated to be an important probe of cellular glycolysis in diseases such as cancer. The usefulness of hyperpolarized ^{13}C imaging is dependent on the relaxation rates of the ^{13}C-enriched substrates, which in turn depend on chemical conformation and properties of the dissolution media such as buffer composition, solution pH, temperature and magnetic field. We have measured the magnetic field dependence of the spin–lattice relaxation time of hyperpolarized [1-^{13}C]pyruvate using field-cycled relaxometry. [1-^{13}C]pyruvate was hyperpolarized using dynamic nuclear polarization and then rapidly thawed and dissolved in a buffered solution to a concentration of 80 mmol l^{-1} and a pH of ~7.8. The hyperpolarized liquid was transferred within 8 s to a fast field-cycling relaxometer with a probe tuned for detection of ^{13}C at a field strength of ~0.75 T. The magnetic field of the relaxometer was rapidly varied between relaxation and acquisition fields where the sample magnetization was periodically measured using a small flip angle. Data were recorded for relaxation fields varying between 0.237 mT and 0.705 T to map the T_1 dispersion of the C-1 of pyruvate. Using similar methods, we also determined the relaxivity of the triarylmethyl radical (OX063; used for dynamic nuclear polarization) on the C-1 of pyruvate at field strengths of 0.001, 0.01, 0.1 and 0.5 T using 0.075, 1.0 and 2.0 mmol l^{-1} concentrations of OX063 in the hyperpolarized pyruvate solution. Copyright © 2012 John Wiley & Sons, Ltd.**

Keywords: dynamic nuclear polarization; relaxation; hyperpolarization; pyruvate

1. INTRODUCTION

Magnetic resonance spectroscopic imaging (MRSI) has been an important tool for molecular imaging with MRI, capable of producing detailed spatial maps of metabolites detected by spectroscopy. Its main drawback is its relatively low sensitivity, which arises from the small polarization of nuclear spins achievable at body temperature (known as thermal polarization) even at fields greater than 3 T. Dynamic nuclear polarization (DNP) is a powerful method used to increase the magnetization of liquid substrates to be used as *in vivo* probes of cellular metabolism with MRSI (1–4). DNP has been used to increase the sensitivity of *in vivo* ^{13}C-spectroscopy of slowly relaxing compounds such as pyruvate (5,6), bicarbonate (7,8), fumarate (9), lactate (10), glutamine (11) and others by more than four orders of magnitude (12). This has led to applications in imaging of vascular disease (13–15), organ perfusion (13,16–18), cancer detection (1,19–22), staging (23,24) and quantification of therapeutic response (2,6,23–26).

DNP is a general method producing enhanced magnetization of most nuclei with non-zero nuclear spin (12). For many nuclei with small gyromagnetic ratios compared with protons, such as ^{13}C, their spin–lattice relaxation time in solution can be tens of seconds long. The slow relaxation is a key physical property that permits *in vivo* detection of these nuclei with MRSI. Several relaxation mechanisms are effective (27). Dipolar relaxation is minimized for carbon positions with no directly attached protons (e.g. carbonyls or carboxylic acids). Dipolar relaxation can be further reduced by full or partial deuteration of the molecule. A deuterated solvent can be chosen to reduce intermolecular dipolar relaxation, but this has little effect *in vivo*. At high magnetic field, chemical shift anisotropy may cause significant relaxation for carbonyls and carboxylic acids in particular. Spin-rotational relaxation may become important for small molecules at higher temperatures. Scalar relaxation of the second kind may cause fast low-field relaxation in molecules where the carbon has a scalar coupling to a quadrupolar nucleus. Finally, paramagnetic impurities should preferably be eliminated or the effect reduced by chelators.

T_1 (spin–lattice relaxation time) can be determined at, for example, 3 T with a suitable pulse sequence to measure the hyperpolarization as a function of time using small-angle RF pulses, but very little data exists for the relaxation of these compounds at low fields, where spin–lattice relaxation could

* *Correspondence to: T. J. Scholl, Imaging Research Laboratory, Robarts Research Institute, Western University, 100 Perth Dr., London, ON, Canada N6A 5K8. E-mail: scholl@uwo.ca*

a *N. Chattergoon, F. Martínez-Santiesteban, T. J. Scholl*
Imaging Research Laboratory, Robarts Research Institute, Western University, 100 Perth Dr., London, ON, Canada N6A 5K8

b *F. Martínez-Santiesteban, T. J. Scholl*
Department of Medical Biophysics, Western University, London, ON, Canada N6A 5C1

c *W. B. Handler*
Department of Physics and Astronomy, Western University, London, ON, Canada N6A 3K7

d *J. H. Ardenkjær-Larsen*
GE Healthcare, Copenhagen, Denmark

e *J. H. Ardenkjær-Larsen*
Department of Electrical Engineering, Technical University of Denmark, Lyngby, Denmark

be significantly faster. Since the hyperpolarized contrast agents are usually dispensed from the DNP apparatus near or at the earth's field, it is important to measure T_1 at these low fields for the exact formulation of the agent that is used for *in vivo* imaging. This includes ^{13}C-enriched substrate concentration, solution pH, buffers and temperature, which all have an effect on relaxation. These data are important to determine key parameters for optimization of the DNP dissolution process and the amount of signal loss that is experienced in transportation from the DNP apparatus to the imaging magnet.

Nuclear magnetic resonance dispersion (NMRD) measurements (T_1 measurements as a function of magnetic field) are typically made using NMR spectrometers by shuttling the sample out of the spectrometer where it is allowed to relax at some field determined by its position in the fringe field of the magnet (28–30). The sample is then rapidly transferred back into the NMR magnet where its remaining magnetization is measured. The process is repeated several times with increasing periods of relaxation at the same point in the magnetic field, building up a relaxation curve, which can be analyzed to estimate T_1. This method is applicable only when the shuttle time is small compared with the relaxation time. Great care must be taken to eliminate stray magnetic fields and determine the average magnetic field that the sample experiences during relaxation. It is worth noting that the shuttling method was used in Mieville *et al.* (28) to measure the T_1 dispersion of hyperpolarized [1-^{13}C]-labeled acetate from 2 mT to 18.8 T, a range that far exceeds that which can be achieved by field-cycling.

Fast field-cycling relaxometry (31–33) is an alternative technique for acquisition of NMRD data. We modified a SpinMaster FFC2000 1 T C/DC (Stelar s.r.l., Italy) fast field-cycling nuclear resonance relaxometer to measure hyperpolarized compounds. Compared with an apparatus using the shuttle method, this instrument is capable of automated NMRD measurements over a more limited range of magnetic fields (0.25 mT to 1 T) by rapidly modulating the current in the resistive magnet of the relaxometer. This permits sample relaxation at a low field and acquisition of the sample free-induction-decay at a fixed higher field (~0.75 T), preserving sensitivity. Since the sample is stationary during these measurements, its temperature can be precisely controlled. The time to transition from relaxation to acquisition field is negligible compared with measured T_1 times and has no systematic effect on these measurements. A custom shim was fitted to the relaxometer to eliminate transverse magnetic fields present arising from components of the relaxometer and surrounding infrastructure. These transverse fields had a significant systematic effect on our T_1 measurements at magnetic fields less than 1 mT.

2. RESULTS AND DISCUSSION

2.1. Measuring T_1

A typical decay curve for hyperpolarized [1-^{13}C]pyruvate is shown in Fig. 1. Each point on the decay curve represents a periodic sampling of the hyperpolarized pyruvate magnetization using a small RF tip angle (5°) to collect a free induction decay measurement at the acquisition field of 0.75 T. The relaxation field for this decay curve was 0.141 T and the repetition time for data acquisition was 3.221 s. The sample temperature was controlled to 37 °C (±0.5 °C). The extracted T_1 for these data, including corrections for tip-angle loss, was 59.8 ± 0.3 s. The R^2-value for this fit was 0.9996 and the uncertainty in T_1 is quoted as a single standard deviation derived from the fitting algorithm assuming even weighting of the decay curve data. The residuals from the non-linear least-squares fit to this decay curve are overlaid as closed triangles.

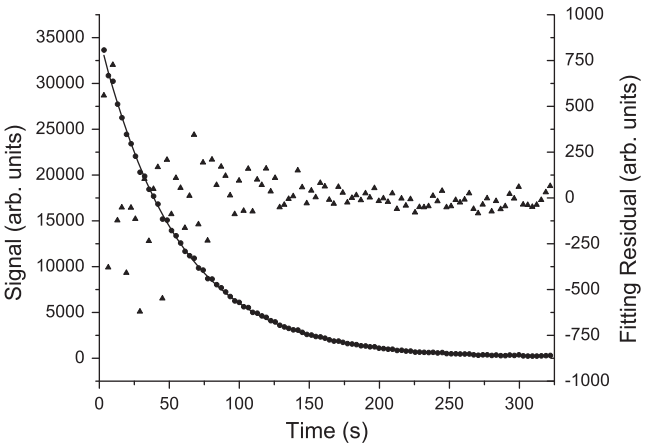

Figure 1. Magnetization decay (solid circles) and fitting model for the C-1 of hyperpolarized [1-^{13}C]pyruvate at a field strength of 0.141 T. The extracted T_1 for these data including corrections for flip-angle loss was 59.8 ± 0.3 s. The R^2-value for this fit was 0.9996. (The uncertainty represents a single standard deviation derived from the non-linear least-squares fitting algorithm assuming even weighting of the decay curve data.) The fitting residuals are plotted as closed triangles.

2.2. T_1 Dispersion and Relaxivity Results

The T_1 results for all 26 measurements are shown in Fig. 2. Measurements were recorded for magnetic fields ranging

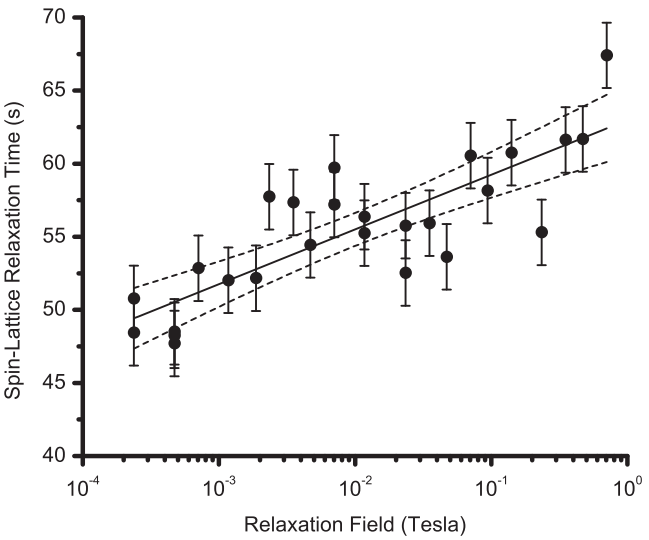

Figure 2. Spin–lattice relaxation time (T_1) for the C-1 of hyperpolarized [1-^{13}C]pyruvate measured at magnetic field strengths between 0.237 mT and 0.705 T. The average statistical uncertainty for determination of T_1 from the decay curves was ±0.33 s (one standard deviation). Repeated T_1 measurements at a particular relaxation field yield a reproducibility of approximately 1.91 s, which is approximately five times larger than the statistical uncertainty quoted above. The fitting results of a model, described in the text, are shown as a solid line. The dashed lines represent 95% confidence bands for this fit.

between 0.237 mT and 0.705 T. The average fitting uncertainty (1 standard deviation) for T_1 was ±0.33 s for all the results. Analysis of the scatter of measurements repeated at a particular relaxation field yielded an experimental reproducibility of approximately 1.91 s for T_1, which is several times larger than the statistical uncertainty quoted above. We conservatively assigned an uncertainty of 2.24 s for all T_1 measurements calculated as the sum of the average statistical uncertainty from all 26 measurements and the experimental reproducibility. The T_1-dispersion data are well characterized by the formula:

$$T_1 = (3.74 \pm 0.52) \times \log_{10}(B_{\text{Relax}}) + (63.0 \pm 1.2)\ \text{s}$$

where B_{Relax} is the relaxation field measured in Tesla. The uncertainties for the fitted parameters represent one standard deviation. The formula is displayed as a solid line in Fig. 2 along with 95% confidence bands (dashed lines). pHs for these samples ranged from 7.63 to 7.93. The average pH measured for these samples was 7.75 with a standard deviation of 0.09. Relaxivity results for OX063-radical-doped pyruvate are given in Table 1. T_1 measurements were made for 1- and 2-mmol l^{-1}-radical concentrations at 0.001, 0.01, 0.1 and 0.5 T using the field-cycled relaxometer. From the T_1 data, the relaxivity of the OX063 radical for the C-1 of pyruvate was calculated at these field points. The relaxivity uncertainties are propagated assuming an uncertainty of 2.24 s for each radical-doped T_1 measurement and from those in the formula characterizing the undoped T_1-dispersion data.

In Fig. 3, the four relaxivity data points are plotted against ^{1}H Larmor frequency. In the same plot we show the water ^{1}H NMRD profile at 23 and 37 °C from Ardenkjaer-Larsen *et al.* (34). The fitting of the ^{1}H dispersion data gave a minimal distance of approach of 5.5 Å and relative translational diffusion constants of 3.4×10^{-9} and 4.2×10^{-9} m^2 s^{-1}, respectively. The ^{13}C relaxivity data points were well approximated by a theoretical NMRD profile calculated with a minimal distance of approach of 7.5 Å and a relative diffusion constant of 2.18×10^{-9} m^2 s^{-1}. The relative diffusion constant was estimated on the basis of the diffusion constant of pyruvate from Schilling *et al.* (35), 0.983×10^{-9} m^2 s^{-1} at 25 °C, which would be approximately 40% higher at 37 °C, i.e. 1.38×10^{-9} m^2 s^{-1}. The diffusion constant of the radical, 0.8×10^{-9} m^2 s^{-1} at 37 °C, was obtained from Ardenkjaer-Larsen *et al.* (34). owing to the limited number of data points, no fitting was attempted.

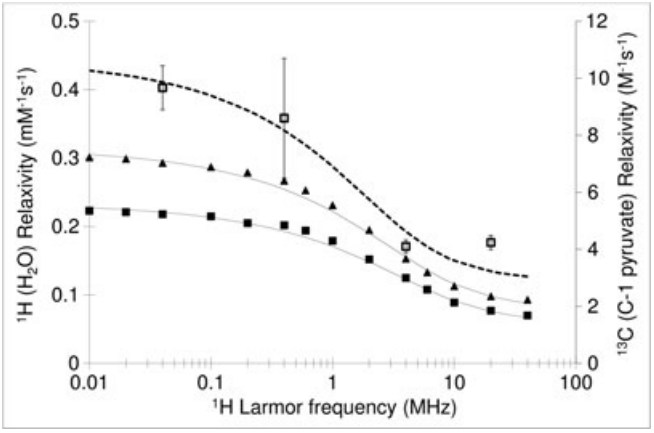

Figure 3. ^{1}H NMRD profiles from Ardenkjaer-Larsen *et al.* (34) for the OX063 TAM radical in water at 23 °C (▲) and 37 °C (■) as a function of ^{1}H Larmor frequency. The fitting of the data provided minimal distance of approach of 5.5 Å and relative diffusion constants of 3.4×10^{-9} and 4.2×10^{-9} m^2 s^{-1}, respectively. In the same graph we show the four data points (□) for the TAM relaxivity towards C-1 of hyperpolarized [1-^{13}C]pyruvate at 37 °C. The dashed curve is the theoretical ^{13}C-pyruvate NMRD using a minimal distance of approach of 7.5 Å and a relative diffusion constant of 2.18×10^{-9} m^2 s^{-1}.

2.3. Experimental Challenges

The buffered pyruvate solution used in these relaxation experiments is a common formulation for *in vivo* animal research (1,2,5,6). Measurement of the T_1 NMRD profile of the C-1 of pyruvate at low-fields provides an estimate of how much hyperpolarized signal is lost as the solution is dispensed at the earth's field and transported to the magnetic resonance imager for injection. Relaxation measurements of long-T_1 compounds are challenging, particularly for low-gyromagnetic nuclei such as ^{13}C. Compared with proton relaxation, the magnetic resonance signals for ^{13}C nuclei at the concentrations used for animal injection are very small and insufficient for relaxometry. The use of DNP to enhance signal acquisition is an obvious resolution to these problems, but presents other experimental challenges. The hyperpolarized solution cannot be re-polarized and, as a result, each datum on the T_1 dispersion curve is from a measurement of a unique sample. This still leads to increased measurement scatter that is apparent in repeated measurements with identical experimental parameters. This is probably due to variations in the dissolution process that

Table 1. Relaxation rates for pyruvate doped with the triarylmethyl radical, OX063. Buffered hyperpolarized [1-^{13}C]pyruvate was combined with a concentrated solution of OX063 to produce 1- and 2-mmol l^{-1}-radical concentrations. The spin–lattice relaxation rates (R_1) were subsequently measured at 0.001, 0.01, 0.1 and 0.5 T. These data were combined with the relaxation rates derived from the undoped pyruvate solution (0.075 mmol l^{-1}) yielding the relaxivity (r_1) of the triarylmethyl radical as a function of magnetic field for the [1-^{13}C] nucleus of pyruvate at 37 °C. The uncertainties quoted in parentheses represent one standard deviation

Magnetic field	R_1 (s^{-1})			r_1
(T)	0.075 mmol l^{-1}	1 mmol l^{-1}	2 mmol l^{-1}	(M^{-1} s^{-1})
0.001	0.01931 (73)	0.0276 (17)	0.0392 (34)	9.68 (77)
0.01	0.01801 (52)	0.0234 (12)	0.0404 (37)	8.6 (2.1)
0.1	0.01687 (37)	0.0204 (9)	0.0250 (14)	4.10 (23)
0.5	0.01616 (32)	0.0206 (9)	0.0241 (13)	4.24 (25)

are difficult to control given its very rapid nature. Subsequent pH measurement of the buffered pyruvate solution is one means of determining variations in the dissolution. Despite careful weighing of stock pyruvate/radical mixture and dissolution medium before insertion in the DNP apparatus to better than a milligram, pHs ranged from 5.5 to 8.3. We chose to reject any T_1 data outside the pH range 7.6–8.0.

Samples were transferred to a pre-warmed (37 °C) NMR tube and quickly carried by hand from polarizer to relaxometer. Temperature and field were not controlled during the brief 8-s transfer time. Transportation has limited influence on the measured T_1 value since T_1 is measured for the sample in magnetic field-controlled environment and temperature of the relaxometer. Conditions during transportation can only affect the amount of hyperpolarization that survives for measurement at the relaxometer. It was not necessary or practical to control the sample exposure to ambient temperature and magnetic field during the brief transfer between polarizer and relaxometer.

Relaxivity measurements of the triarylmethyl (TAM) radical rely on accurate knowledge of its concentration in the buffered pyruvate solution. The concentrated TAM–water solution can be carefully pipetted into the NMR tube and weighed; however, relaxation of the pyruvate solution after dissolution affords only enough time for rapid pipetting of this solution into the TAM-containing NMR tube and gentle agitation of the combined solution as the sample is rushed to the relaxometer. Repeated relaxation measurements at a given TAM concentration suggest that the variability in the resulting relaxation time constant is no larger than that observed for the T_1-dispersion measurements, indicating that this procedure is sufficiently accurate for these purposes.

Long acquisition times for the magnetization decay curve (300–500 s) required control of the sample temperature. This was accomplished by dispensing the solution into a pre-warmed NMR tube before insertion into the relaxometer. Temperature-regulated air (37 °C) was blown around the sample tube during relaxation measurement.

3. CONCLUSIONS

Low-field relaxation of [1-^{13}C]pyruvate was measured in solution using field-cycled relaxometry and dynamic nuclear polarization for sensitivity enhancement. The T_1-dispersion of a hyperpolarized solution of buffered pyruvate was measured from 0.237 mT and 0.705 T at a temperature of 37 °C (±0.5 °C). This solution was a common formulation for *in vivo* animal research (1,2,5,6). Analysis of the results showed that the relaxation time for the C-1 nucleus was ~46.9 s at the earth's magnetic field (0.05 mT) compared with ~65 s at 3 T, a decrease of 28%. For our infrastructure, the time interval required to dispense the hyperpolarized pyruvate solution and transfer it to the magnetic resonance scanner was ~8 s. Assuming that the solution spends most of its time at the earth's field during this interval, one calculates that approximately 16% of the sample magnetization is lost during transfer. One could devise a system where the hyperpolarized solution was dispensed into a holding field (instead of the earth's field) in which the hyperpolarized solution could be transferred to the fringe field of the imaging magnet. A modest holding field of 0.01 T would increase the T_1 of the pyruvate solution by nearly 18%; however, for a relatively short transfer time of 8 s, these measurements suggest that one could only achieve a 2.3% increase in signal intensity by this added complexity. For longer transfer times or compounds with greater T_1 dispersion, a transfer field might be a worthwhile effort.

The relaxivity of the TAM radical, OX063, on the C-1 carbon was measured using field-cycled relaxometry for magnetic fields less than 1 T. The relaxivity of this paramagnetic compound ranged from 9.68(77) $\text{M}^{-1}\,\text{s}^{-1}$ at a magnetic field strength of 1 mT to 4.24(25) $\text{M}^{-1}\,\text{s}^{-1}$ at 0.5 T. This is about 30 times lower than the water proton relaxivity, which is mainly due to the lower gyromagnetic ratio of ^{13}C (accounting for 16-times-lower relaxivity) and the larger size of pyruvate compared with water. The TAM radical was added to pyruvic acid at a concentration of 15 mmol l^{-1}. After dissolution, the concentration was approximately 75 μM so that, at a field strength of 1 mT, the presence of the radical shortened the T_1 of the hyperpolarized buffered pyruvate solution by 2 s. Removal of the radical after dissolution by filtering is possible but the benefit of only a modest decrease in relaxation rate would not make this worthwhile based on the additional time requirement for that process. However, for other substances that are hyperpolarized in a solvent at a lower effective concentration than pyruvic acid (such as bicarbonate (8) or fumaric acid (9)), this additional relaxation could be a significant concern at low fields, since after dissolution the radical ends up at a higher concentration (than for polarization of pyruvate) for the same concentration of the ^{13}C-labeled compound.

4. EXPERIMENTAL METHODS

4.1. Sample Preparation

A DNP apparatus (HyperSense, Oxford Instruments, Abingdon UK) was used to hyperpolarize [1-^{13}C]pyruvic acid (Cambridge Isotope Laboratories, Cambridge, MA, USA). Following a preparation that is widely used for *in vivo* research (1,2,5,6), approximately 30 mg of a mixture of [1-^{13}C]pyruvic acid and 15-mmol l^{-1} OX063 triarylmethyl radical (Oxford Instruments Molecular Biotools, Abingdon UK) were precisely weighed in a sample cup and inserted in the DNP apparatus for polarization over approximately 1 h. Dissolution medium was prepared using a solution of 40-mmol l^{-1} Trizma Pre-Set Crystals (pH 7.6, Sigma Aldrich, St Louis, MO, USA) and 80-mmol l^{-1} sodium hydroxide in de-ionized water. Disodium ethylenediaminetetraacetic acid was added at a concentration of 100 mg l^{-1} to sequester any metal ion contamination that might arise from contact between the dissolution medium and the DNP dissolution fluid path. Immediately prior to dissolution, the DNP apparatus was loaded with ~4.55 ml of the dissolution medium calculated to produce a concentration of 80-mmol l^{-1} pyruvate upon dissolution at a pH of ~7.75 and temperature of ~40 °C. The dissolution medium was not degassed and no effort to purge the pathway of oxygen was attempted. The buffered hyperpolarized pyruvate was dispensed into a pear-shaped flask and 1.1 ml of the liquid was drawn up into a syringe, transferred to a pre-warmed 10-mm-diameter NMR tube and rapidly transported to the field-cycling relaxometer. Typical polarization times were ~45 min producing better than 15% polarization of the pyruvate solution.

As a check for possible systematic experimental effects, the remaining aliquot of every pyruvate dissolution was dispensed into a 0.55 T benchtop NMR spectrometer (Oxford Instruments Magnetic Resonance, Abingdon, UK). The spectrometer was programmed to measure the T_1 relaxation at 37 °C using a small

flip angle (5°) excitation pulse and 5-s repetition time for 100 acquisitions at this single field strength. After each measurement, the pH of samples from both the bench-top spectrometer and the field-cycling relaxometer were recorded. It should be noted here that each T_1 measurement is a separate hyperpolarization dissolution from the DNP apparatus. Care was taken to assure measurement-to-measurement reproducibility of the sample composition by careful weighing of all sample components including dissolution medium.

4.2. Relaxivity Measurements of TAM Radical

For determination of the effects of the TAM radical on pyruvate relaxation, a stock solution of 100-mmol l^{-1} OX063 dissolved in de-ionized water was prepared. Prior to dissolution of the hyperpolarized pyruvic acid, a small volume (10 or 20 μl) of the OX063/water preparation was placed into the bottom of a NMR tube. A 1000-μl aliquot of 80-mmol l^{-1} hyperpolarized pyruvate solution (described above) was rapidly pipetted from the catch flask into the NMR tube and mixed by moderate shaking to produce either 1 or 2 mmol l^{-1} of OX063 in the combined solution. T_1 was measured for these two concentrations at four magnetic field strengths (0.001, 0.01, 0.1 and 0.5 T) using the field-cycling relaxometer.

4.3. Relaxometry

The field-cycling relaxometer was located in an adjacent laboratory approximately 26 m from the DNP apparatus. This distance was traversed in approximately 8 s, running with the sample in hand. All three components of the magnetic field were roughly surveyed along this route at 1-m intervals. The magnitude of the ambient field varied between 0.022 and 0.082 mT with an average of 0.045 mT. The direction of the field was primarily vertical ($B_{vertical}/B_{magnitude} \approx 0.75$) and the vertical component of the magnetic field did not change direction along the trajectory.

The relaxometer was programmed to measure the sample magnetization 100 times with a fixed repetition time (typically 3–5 s) with a small flip angle (5°). The magnitude of each FID was integrated to produce the magnetization as a function of time. The spin–lattice relaxation time was extracted from a three-parameter exponential model using a standard non-linear least-squares fitting algorithm implemented in MATLAB (MathWorks, Natick, MA, USA) assuming even weighting for all data:

$$\text{signal} = A\cos^{(n-1)}(\alpha)e^{-nT_R/T_1} + y_0$$

where A is the initial signal amplitude (y-intercept), T_1 is the spin–lattice relaxation time and y_0 is the signal offset.

The term, $\cos^{(n-1)}(\alpha)$, is a correction for loss of longitudinal magnetization at the nth measurement for a flip angle, α. This angle was pre-determined by calibration and the repetition time, T_R, was also fixed at its known value. The temperature of the sample was maintained at 37 °C (± 0.5 °C) using heated air during the experiment. The relaxometer was typically set up for acquisition of the ^{13}C signal at a field strength of 0.75 T with 100-ms-ramp time between relaxation and acquisition fields. After insertion of the sample into the relaxometer, the pulse sequence was manually started from the NMR console.

We designed and fitted a transverse field shim to the relaxometer to cancel any non-axial fields owing to components of the relaxometer itself and external influences such as laboratory infrastructure. At the lowest relaxation fields, stray fields are significant, producing a net relaxation field different from the specified field and not parallel to the acquisition field direction. This effectively produces an unaccounted loss of sample magnetization during field-cycling between acquisition and relaxation fields. This is a potential source of systematic error for measurement of the decay of hyperpolarized compounds, which involves absolute measurement of magnetization and is not a consideration for relaxometry of thermally polarized agents where the sample magnetization is re-established before each relaxation period. Our initial NMRD data without shim correction showed a 'knee' in the dispersion curve data around 1 mT. Measured relaxation data at lower fields were systematically less than those we ultimately reported here and the discrepancy increased with decreasing field. By 0.7 mT, this systematic effect was responsible for a 30 s reduction in the relaxation time. To mitigate this effect, a cylindrical shim was designed on a radius of 7.064 cm and was concentric with the field-cycling magnet, and fastened around the acrylic cooling sleeve. The azimuthal orientation and strength of the shim was determined by insertion of a three-axis Hall-effect probe (Senis GmbH., Zurich, Switzerland) that was placed in the sample probe of the spectrometer. This shim reduced the transverse component of the stray magnetic field from ~0.1 mT to less than 0.01 mT (measurement limit for probe) for a shim current of 1.0 A.

Calibration of the flip angle was an important aspect of the experimental measurement. For this work, α was calibrated using a phantom of [1-^{13}C]pyruvic acid doped with ProHance (Gadoteridol, Gd-HP-DO3A, Bracco Diagnostics Inc.) to reduce the T_1 of the ^{13}C nuclei to ~175 ms. This phantom was identical in volume with the hyperpolarized pyruvate samples. A series of measurements were undertaken to determine the RF pulse width corresponding to a flip angle of 90 and 180° for both ^{1}H and ^{13}C nuclei. Pulse widths scaled with angle and inversely with respect to the gyromagnetic ratios of the two nuclei, as expected.

Acknowledgements

The authors would like to thank the Ontario Institute for Cancer Research, Imaging Translation Program and the Natural Sciences and Engineering Research Council of Canada for funding this research. We also like to acknowledge useful discussions with Albert Chen, GE Healthcare, Toronto, Canada, Gianni Ferrante, Stelar s.r.l., Italy, and William Mander, Oxford Instruments, UK.

REFERENCES

1. Ardenkjaer-Larsen JH, Golman K, in't Zandt R, Lerche M, Pehrson R. Metabolic imaging by hyperpolarized C-13 magnetic resonance imaging for in vivo tumor diagnosis. Cancer Res 2006;66 (22):10855–10860.
2. Brindle KM, Witney TH. Imaging tumour cell metabolism using hyperpolarized (13)C magnetic resonance spectroscopy. Biochem Soc Trans 2010;38:1220–1224.
3. Kurhanewicz J, Vigneron DB, Brindle K, Chekmenev EY, Comment A, Cunningham CH, Deberardinis RJ, Green GG, Leach MO, Rajan SS, Rizi RR, Ross BD, Warren WS, Malloy CR. Analysis of cancer metabolism by imaging hyperpolarized nuclei: prospects for translation to clinical research. Neoplasia 2011;13(2):81–97.
4. Petersson JS, Golman K, Magnusson P, Johansson E, Akeson P, Chai CM, Hansson G, Mansson S. Cardiac metabolism measured noninvasively by hyperpolarized C-13 MRI. Magnet Reson Med 2008;59 (5):1005–1013.
5. Golman K, in't Zandt R, Thaning M. Real-time metabolic imaging. Proc Natl Acad Sci USA 2006;103(30):11270–11275.

6. Brindle KM, Day SE, Kettunen MI, Cherukuri MK, Mitchell JB, Lizak MJ, Morris HD, Matsumoto S, Koretsky AP. Detecting response of rat C6 glioma tumors to radiotherapy using hyperpolarized [1-(13)C]pyruvate and (13)C magnetic resonance spectroscopic imaging. Magnet Reson Med 2011;65(2):557–563.
7. Brindle KM, Gallagher FA, Kettunen MI, Day SE, Hu DE, Ardenkjaer-Larsen JH, in't Zandt R, Jensen PR, Karlsson M, Golman K, Lerche MH. Magnetic resonance imaging of pH in vivo using hyperpolarized (13)C-labelled bicarbonate. Nature 2008;453(7197):940–973.
8. Wilson DM, Keshari KR, Larson PE, Chen AP, Hu S, Van Criekinge M, Bok R, Nelson SJ, Macdonald JM, Vigneron DB, Kurhanewicz J. Multi-compound polarization by DNP allows simultaneous assessment of multiple enzymatic activities in vivo. J Magn Reson 2010;205 (1):141–147.
9. Brindle KM, Gallagher FA, Kettunen MI, Hu DE, Jensen PR, in't Zandt R, Karlsson M, Gisselsson A, Nelson SK, Witney TH, Bohndiek SE, Hansson G, Peitersen T, Lerche MH. Production of hyperpolarized [1,4-(13)C(2)]malate from [1,4-(13)C(2)]fumarate is a marker of cell necrosis and treatment response in tumors. Proc Natl Acad Sci USA 2009;106(47):19801–19806.
10. Chen AP, Kurhanewicz J, Bok R, Xu D, Joun D, Zhang V, Nelson SJ, Hurd RE, Vigneron DB. Feasibility of using hyperpolarized [1-13C]lactate as a substrate for in vivo metabolic 13C MRSI studies. Magn Reson Imag 2008;26(6):721–726.
11. Brindle KM, Gallagher FA, Kettunen MI, Day SE, Lerche M. C-13 MR spectroscopy measurements of glutaminase activity in human hepatocellular carcinoma cells using hyperpolarized C-13-labeled glutamine. Magnet Reson Med 2008;60(2):253–257.
12. Ardenkjaer-Larsen JH, Fridlund B, Gram A, Hansson G, Hansson L, Lerche MH, Servin R, Thaning M, Golman K. Increase in signal-to-noise ratio of >10,000 times in liquid-state NMR. Proc Natl Acad Sci USA 2003;100(18):10158–10163.
13. Ishii M, Emami K, Kadlecek S, Petersson JS, Golman K, Vahdat V, Yu JS, Cadman RV, MacDuffie-Woodburn J, Stephen M, Lipson DA, Rizi RR. Hyperpolarized C-13 MRI of the pulmonary vasculature and parenchyma. Magnet Reson Med 2007;57(3):459–463.
14. Lau AZ, Chen AP, Cunningham CH. Integrated Bloch-Siegert B(1) mapping and multislice imaging of hyperpolarized (13) C pyruvate and bicarbonate in the heart. Magn Reson Med 2012;67(1):62–71.
15. Lau AZ, Chen AP, Ghugre NR, Ramanan V, Lam WW, Connelly KA, Wright GA, Cunningham CH. Rapid multislice imaging of hyperpolarized 13C pyruvate and bicarbonate in the heart. Magn Reson Med 2010;64 (5):1323–1331.
16. Golman K, Ardenaer-Larsen JH, Petersson JS, Mansson S, Leunbach I. Molecular imaging with endogenous substances. Proc Natl Acad Sci USA 2003;100(18):10435–10439.
17. Johansson E, Mansson S, Wirestam R, Svesson J, Petersson S, Golman K, Stahlberg F. Cerebral perfusion assessment by bolus tracking using hyperpolarized C-13. Magnet Reson Med 2004;51(3):464–472.
18. Johansson E, Olsson LE, Mansson S, Petersson JS, Golman K, Stahlberg F, Wirestam R. Perfusion assessment with bolus differentiation: a technique applicable to hyperpolarized tracers. Magnet Reson Med 2004;52(5):1043–1051.
19. Albers MJ, Bok R, Chen AP, Cunningham CH, Zierhut ML, Zhang VY, Kohler SJ, Tropp J, Hurd RE, Yen YF, Nelson SJ, Vigneron DB, Kurhanewicz J. Hyperpolarized 13C lactate, pyruvate, and alanine: noninvasive biomarkers for prostate cancer detection and grading. Cancer Res 2008;68(20):8607–8615.
20. Chen AP, Albers MJ, Cunningham CH, Kohler SJ, Yen YF, Hurd RE, Tropp J, Bok R, Pauly JM, Nelson SJ, Kurhanewicz J, Vigneron DB. Hyperpolarized C-13 spectroscopic imaging of the TRAMP mouse at 3 T-initial experience. Magn Reson Med 2007;58(6): 1099–1106.
21. Lupo JM, Chen AP, Zierhut ML, Bok RA, Cunningham CH, Kurhanewicz J, Vigneron DB, Nelson SJ. Analysis of hyperpolarized dynamic 13C lactate imaging in a transgenic mouse model of prostate cancer. Magn Reson Imag 2010;28(2):153–162.
22. Vigneron DB, von Morze C, Larson PEZ, Hu S, Keshari K, Wilson DM, Ardenkjaer-Larsen JH, Goga A, Bok R, Kurhanewicz J. Imaging of blood flow using hyperpolarized [(13)C] urea in preclinical cancer models. J Magn Reson Imag 2011;33(3):692–697.
23. Brindle KM, Bohndiek SE, Gallagher FA, Kettunen MI. Tumor imaging using hyperpolarized (13)C magnetic resonance. Magnet Reson Med 2011;66(2):505–519.
24. Park I, Bok R, Ozawa T, Phillips JJ, James CD, Vigneron DB, Ronen SM, Nelson SJ. Detection of early response to temozolomide treatment in brain tumors using hyperpolarized 13C MR metabolic imaging. J Magn Reson Imag 2011;33(6):1284–1290.
25. Brindle KM, Bohndiek SE, Kettunen MI, Hu DE, Witney TH, Kennedy BWC, Gallagher FA. Detection of tumor response to a vascular disrupting agent by hyperpolarized (13)C magnetic resonance spectroscopy. Mol Cancer Ther 2010;9(12):3278–3288.
26. Brindle KM, Witney TH, Kettunen MI, Hu DE, Gallagher FA, Bohndiek SE, Napolitano R. Detecting treatment response in a model of human breast adenocarcinoma using hyperpolarised [1-(13)C]pyruvate and [1,4-(13)C(2)]fumarate. Br J Cancer 2010;103(9):1400–1406.
27. Levitt MH. *Spin Dynamics: Basics of Nuclear Magnetic Resonance*. Wiley: Chichester, 2001.
28. Mieville P, Jannin S, Bodenhausen G. Relaxometry of insensitive nuclei: optimizing dissolution dynamic nuclear polarization. J Magn Reson 2011;210(1):137–140.
29. Redfield AG. Shuttling device for high-resolution measurements of relaxation and related phenomena in solution at low field, using a shared commercial 500 MHz NMR instrument. Magn Reson Chem 2003;41(10):753–768.
30. Grosse S, Gubaydullin F, Scheelken H, Vieth HM, Yurkovskaya AV. Field cycling by fast NMR probe transfer: Design and application in field-dependent CIDNP experiments. Appl Magn Reson 1999;17 (2–3):211–225.
31. Kimmich R, Anoardo E. Field-cycling NMR relaxometry. Prog Nucl Mag Reson Spectrosc 2004;44(3–4):257–320.
32. Baroni S, Bubici S, Ferrante G, Aime S. in *Magnetic Resonance in Food Science: Challenges in a Changing World*. (Eds: M. Guojonsdottir, P.S. Belton, G.A. Webb), Royal Chemistry Society: Cambridge, UK, 2009; pp. 65–72.
33. Anoardo E, Galli G, Ferrante G. Fast-field-cycling NMR: applications and instrumentation. Appl Magn Reson 2001;20(3):365–404.
34. Ardenkjaer-Larsen JH, Laursen I, Leunbach I, Ehnholm G, Wistrand LG, Petersson JS, Golman K. EPR and DNP properties of certain novel single electron contrast agents intended for oximetric imaging. J Magn Reson 1998;133(1):1–12.
35. Schilling FDS, Durst M, Kollisch U, Ardenkjaer-Larsen JH, Gomez Damian PA, Schwaiger M, Shulte RF, Glaser SJ, Haase A, Otto A, Menzel MI. *Proceedings of the International Society for Magnetic Resonance in Medicine 20th Scientific Meeting*. Melbourne, May 2012, p. 1683a.